Manifestations of Static and Dynamic Heterogeneity in Single Molecule Translational Measurements in Glassy Systems

Nicole L. Mandel[+], Talha Rehman[+,#], and Laura J. Kaufman*

Department of Chemistry, Columbia University, New York, New York, USA.

[#]current address: John A. Paulson School of Engineering and Applied Sciences, Harvard University, Cambridge, MA, USA

[+]these authors contributed equally to this work

*corresponding author: kaufman@chem.columbia.edu

Abstract

Rotational-translational decoupling in systems near T_g, in which translational diffusion is apparently enhanced relative to rotation, has been observed in ensemble and single molecule experiments and has been linked to dynamic heterogeneity. Here, simulations of single molecules experiencing homogeneous diffusion and static and dynamic heterogeneous diffusion are performed to clarify the contributions of heterogeneity to such enhanced translational diffusion. Results show that time-limited trajectories broaden the distribution of diffusion coefficients in the presence of homogeneous diffusion but not when physically reasonable degrees of static heterogeneity are present. When dynamic heterogeneity is introduced, measured diffusion coefficients uniformly increase relative to input diffusion coefficients, and the widths of output distributions decrease, providing support for the idea that dynamic heterogeneity can drive apparent translational enhancement. Among simulations with dynamic heterogeneity, when frequency of dynamic exchange is correlated with initial diffusion coefficient, measured diffusion coefficient behavior as a function of observation time matches that seen experimentally, the only set of simulations explored in which this occurs. Taken together with experimental results, this suggests enhanced translational diffusion in glassy systems occurs through dynamic exchange consistent with wide underlying distributions of diffusion coefficients and exchange coupled to local spatiotemporal dynamics.

Introduction

The dynamics of glass formers near their glass transition temperatures (T_g) has been investigated for decades both in experiment[1–3] and simulation.[4–12] One particularly interesting aspect of glass formers near T_g is their apparent dynamic heterogeneity, with many experimental observations suggesting the presence of a wide distribution of timescales that vary as a function of space and time in such systems.[1–3,12–17] Dynamic heterogeneity is a phenomenon of considerable interest for its potential causal relationship with other unusual properties seen in glassy systems, including the non-Arrhenius temperature dependence of viscosity and the violation of the Stokes-Einstein (SE) and Debye-Stokes-Einstein (DSE) behavior in glassy systems.

The SE and DSE relationships relate translational (D_T) and rotational diffusion (D_r) coefficients to system viscosity via $D_T = \frac{kT}{6\pi\eta r_s}$ and $D_r = \frac{kT}{8\pi\eta r_s^3}$, where T is temperature, r_s is hydrodynamic radius of a tracer particle, and η is viscosity. Experimentally, rotational dynamics and DSE behavior are most commonly quantified through rotational relaxation time, τ_c, via $\tau_c = \frac{4\pi\eta r_s^3}{3kT}$. While the SE and DSE relationships predict that the translational diffusion coefficient, D_T, and the inverse rotational correlation time, τ_c^{-1}, will both scale with T/η, deviations from this prediction have been found across many glassy systems. with D_T typically showing a weaker temperature dependence than τ_c^{-1} as T_g is approached from above.[2,3,18–25] [5,6,8,11,12,26–28] These systems display apparent rotational-translational decoupling and translational enhancement.

Deviations from SE and DSE behavior have been interpreted in the context of dynamic heterogeneity, with the hypothesis that measurements of D_T more heavily weight fast dynamics while measurements of τ_c do so for slow dynamics.[1–3] Recently, we showed experimentally that rotational-translational decoupling persists on a single molecule level and cannot be ascribed solely to ensemble averaging over a heterogeneous system.[13] In particular, when fluorescent probe molecules were dispersed in high molecular weight polystyrene near T_g and these probes were simultaneously monitored for rotational and translational dynamics, a significant degree of enhanced translational dynamics relative to rotational dynamics was seen for most individual molecules.[13] These findings suggest that a combination of averaging over molecules with distinct, non-evolving dynamics and over molecules with rapidly changing dynamics contributes to ensemble observations of rotational-translational decoupling.

Here, given our recent measurements showing enhanced translational motility at the single molecule level, we perform simulations analogous to earlier ones that facilitated interpretation of single molecule experiments of rotational dynamics in supercooled

liquids.[29,30] In particular, we investigate how typical experimental constraints in the context of heterogeneity with both slow (non-evolving on the experimental timescale, or static) and fast (dynamic) exchange manifests in measured observables. In experiments, individual probe molecule trajectories were found to yield mean square displacements (MSDs) that grow linearly in time, consistent with diffusive behavior over the time scales assessed.[13,31,32] From these MSDs, wide breadths of translational diffusion coefficients were found across molecules, suggestive of significant (static) heterogeneity.[13,31] However, the persistence of rotational-translational decoupling in single molecule measurements suggests a significant degree of dynamic heterogeneity is also present. Here, we present simulations of particles experiencing homogeneous translational diffusion and heterogeneous (static and dynamic) translational diffusion with limited trajectory lengths as may occur experimentally due to photobleaching, out-of-plane rotation, or errors in particle tracking along with realistic levels of noise, which can lead to errors in particle localization, to understand the effects of these factors on analysis and interpretation of translational trajectories. We find, as in single molecule rotational analysis,[29,30] degeneracies in observables for homogeneous systems and those with fast dynamic exchange, complicating identification of timescales of dynamic exchange. Interestingly, we also find that an unexpected experimental observation is reproduced in simulations when dynamic exchange is coupled to local dynamics, suggesting this is likely a feature of dynamic heterogeneity in glassy systems.

Methods

Simulations of Translational Diffusion

Two dimensional (2D) Monte Carlo simulations of Brownian motion were performed on custom-modified National Instruments LabView software originally described in Ref. [33] and expanded upon in References [34] and [35]. Video frames were simulated by seeding approximately 100 point features that represent fluorescent probe molecules on a grid across 512 x 512 pixels representing an area consistent with an experimental pixel size of 169 nm, as used for data collected in Ref. 13. Simulated molecules were set in an ordered array to reduce the likelihood of molecules crossing paths, which could lead to tracking errors that do not typically occur experimentally, and simulated molecules were set to persist through the full movie (35 to 2000 frames). The range of frame number investigated was chosen (1) to represent typical number of frames found for individual molecules in Reference 13, which typically ranged between 30-200 frames and (2) to assess the impact of longer trajectory lengths on assessed observables to investigate possible limited trajectory length effects in experimental and simulated data. All features were simulated as bright spots with a Gaussian intensity profile with FWHM of 294 nm,

consistent with typical optical diffraction in single molecule imaging. The time between simulated frames (TBF) was set between 1 and 40 seconds to capture the majority of experimental TBFs (which ranged between 0.4-120s) as described in Reference 13. Brownian diffusion was simulated by assigning step sizes frame-by-frame from a Gaussian probability distribution generated based on each molecule's assigned diffusion coefficient in x and y dimensions. The probability that a molecule will take a step between x and x+Δx is given by: $P(x)\Delta x = (1/\sigma\sqrt{2\pi})\, e^{(-x^2/2\sigma^2)}\Delta x$, where $\sigma = \sqrt{2Dt}$, with D the assigned diffusion coefficient and t the time.

Most simulations were performed without background signal or noise, with signal level set arbitrarily to 100. Performing analysis on static features simulated in this manner showed no localization inaccuracy, returning exclusively 0 step sizes and diffusion coefficients. To mimic the effect of noise in the experiment described in Reference 13, some simulations included stochastic noise, added to each pixel with a standard deviation equal to the square root of the pixel intensity. In these simulations, average signal intensity was adjusted in the presence of this stochastic noise to reproduce apparent diffusion coefficients obtained from experimental tracking of molecules far below the glass transition temperature, where all motion was attributed to localization error.[13] This resulted in, for simulations in which the features are not moving, median apparent step sizes of 15 nm (as compared to 8.6 nm obtained from experimental measurements described in Ref. 13) and median apparent positive diffusion coefficients of 0.45 nm^2s^{-1} (compared to 0.47 nm^2s^{-1} in experiment), with approximately 54% of molecules returning apparently negative diffusion coefficients (compared to 26% in experiment). We thus deem this approach sufficiently consistent with experimental movies far below T_g, where molecules are likewise expected to be static.[13] Simulations including both stochastic noise as described above plus additional background intensity, which itself has stochastic noise, were also performed. Here background intensity values were set to be "moderate" or "high" to mimic background intensity similar to but somewhat higher than that in experiments. Signal to background (S:B) ratios in experiments described in Ref. 13 for 2s exposure were approximately 4.5, and the above background settings led to simulated S:B ratios of 2.8 and 1.4, respectively. These settings resulted in, for static particle simulations, median step sizes of 19 and 23 nm, and median positive diffusion coefficients of 1.06 and 1.08 nm^2s^{-1}, with 55 and 31% of molecules found to have negative diffusion coefficients, respectively. These results indicate that simulations with both moderate and high levels of background signal exhibit somewhat lower localization accuracy than the experiments described in Ref. 13.

Diffusion coefficients were assigned to simulated molecules to mimic homogeneous, statically heterogeneous, dynamically heterogeneous, or correlated (D-dependent) dynamically heterogeneous dynamics (Fig. 1). In the homogeneous case, a single

diffusion coefficient was assigned to every molecule, and the diffusion coefficient was retained for the entirety of the simulated movie. In the spatially heterogeneous (static) case, molecules were randomly assigned a diffusion coefficient from a log normal distribution centered at D_{set} and with σ the set standard deviation on a log scale. This diffusion coefficient was retained for the entirety of the simulated movie. The width of this seed distribution will subsequently be referred to in terms of the set standard deviation, σ. In the dynamically heterogeneous case, simulated molecules were assigned initial diffusion coefficients as in the static heterogeneity case, but after a set number of frames molecules were randomly re-assigned diffusion coefficients from a distribution with the same median and width as the original distribution. All molecules in this case changed their diffusion coefficients at the same frame and experienced the same number of dynamical exchanges per movie. For D-dependent exchange, molecules were assigned initial diffusion coefficients as in the static and dynamic heterogeneity cases, but the number of frames before their subsequent exchange was determined by: $Fr_{ex} = Fr_{med} - [\log(D_c/D_{med}) * 10]$, where Fr_{med} is the set median number of frames before exchange, D_c is the current assigned diffusion coefficient, and D_{med} is the set median diffusion coefficient, both in nm^2/sec. In practice, in these simulations this results in a 10 frame difference before exchange for each order of magnitude difference in diffusion coefficient. Median set diffusion coefficients were 1 and 10 nm^2s^{-1}, covering a portion of the range explored in Reference 13. For systems with heterogeneity present, individual molecule D_{set} varied between 0.0001-10000 nm^2s^{-1}, depending on median D_{set} and degree of heterogeneity (σ = 0.1, 0.2, 0.8, 1) explored in a particular simulation.

For D-dependent exchange, in order to simulate longer times between frames (TBF) for a given number of exchanges, total movie length and median movie length between exchanges were set in accordance with the TBF. For example, for the 4s TBF movies, maximum movie length was 100 frames, and the median number of frames for the diffusion coefficient to persist before exchange was set to 20; in contrast, for movies with 16s TBF, maximum movie length was set to 25 frames, and the median number of frames for the diffusion coefficient to persist before exchange was set to 5. Thus, in both movies, a molecule assigned the median diffusion coefficient would maintain that diffusion coefficient for 80 seconds before dynamic exchange. This replicates the TBF conditions for experimental movies, as movies were extended to longer TBFs by removing intermediate frames, meaning that total trajectory length in seconds was held constant.[13]

Exemplary simulated movies with static heterogeneity with median D_{set} =10 nm^2/s and a wide distribution (σ = 1) with and without noise set to match that in experiments are provided as Supplementary Movies 1 and 2. In both cases, images were generated every 4 seconds (TBF = 4s).

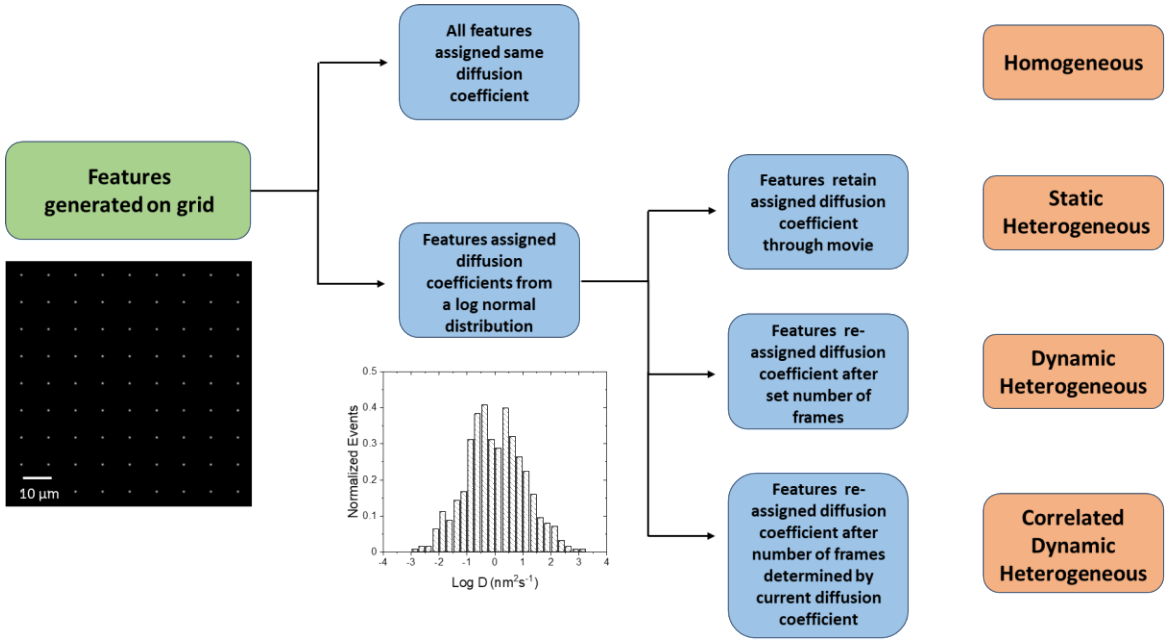

Figure 1. Schematic depiction of simulations highlighting differences between homogeneous, static heterogeneous, and dynamic heterogeneous implementations. An exemplary distribution of input timescales is shown for heterogeneous simulations.

Data Analysis

Simulated movies were analyzed using TrackPy software.[36] Features were tracked frame by frame[37] and trajectories were used to calculate time averaged mean square displacements via $MSD(\tau) \equiv < [r(t+\tau) - r(t)]^2 > = < (x(t+\tau) - x(t))^2 + (y(t+\tau) - y(t))^2 >$, where τ is lag time. MSD was then plotted against lag time and fit by linear regression to $MSD = 4\mathrm{D}t + \varepsilon$, where $\varepsilon \approx 4\sigma^2$, and σ is localization error (Fig. 2). The first 6 lag times were used to calculate diffusion coefficients to avoid long-lag time error associated with poor statistics at those lag times. The same approach was used in recent analysis of the experiments on which these simulations are modeled.[13]

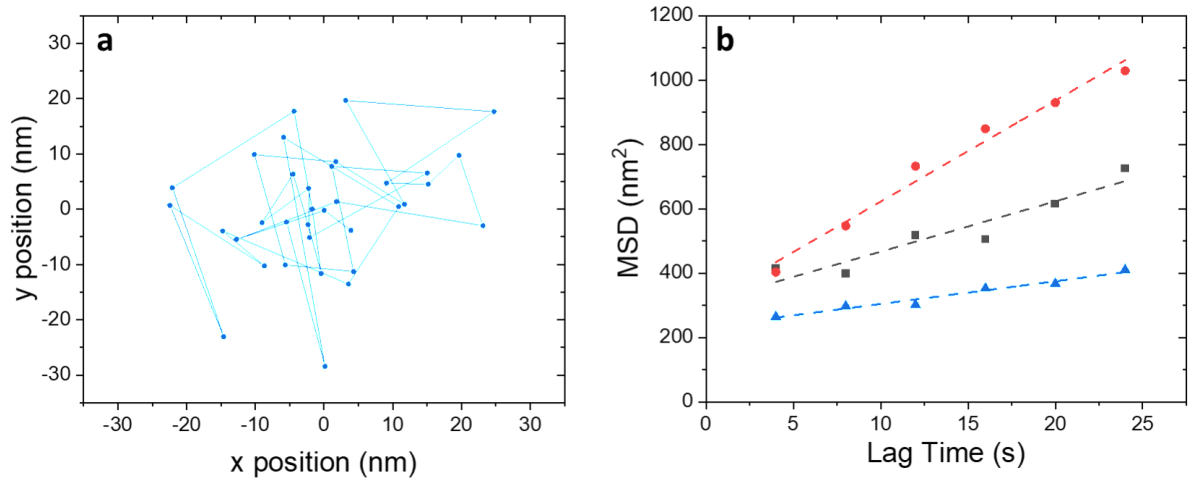

Figure 2. (a) Representative generated trajectory for a simulated single molecule with output D = 1.8 nm^2/s and frames generated every 4 seconds for 35 frames. (b) Representative MSD vs. lag time values and associated fits for 3 simulated molecules from a static heterogeneous simulation with a wide distribution of diffusion coefficients (σ = 1), 4s between frames, median D_{set} = 1 nm^2/s. Different colors indicate different simulated features, with blue the MSD associated with the trajectory presented in (a). Best fits return the following parameters: red, m=31.4 nm^2/s, b=308 nm^2, R^2=0.98, yielding D=7.9 nm^2/s; black, m=15.7 nm^2/s, b=310 nm^2, R^2=0.89, yielding D=3.9 nm^2/s; blue, m=7.06 nm^2/s, b=233 nm^2/s, R^2=0.97, yielding D=1.8 nm^2/s. The simulation was performed with stochastic molecule noise and no background signal.

Results and Discussion

Homogeneous and Heterogeneous Simulations Without Noise

Simulations of single molecules exhibiting homogeneous, static heterogeneous, and dynamic heterogeneous translational dynamics were first performed without noise. Even without noise similar to that present in experiments explicitly included, potential errors and biases inherent to the tracking analysis and diffusion coefficient calculations may be present.

For simulations of homogeneous diffusion without noise or background, Fig. 3 demonstrates that increasing trajectory length (for a given TBF) has little effect on apparent median diffusion coefficient (Fig. 3a). The effect is somewhat less obvious than in analysis of rotational correlation times in single molecule measurements and simulations, where trajectories shorter than ≈ 100 times the rotational correlation time demonstrate obvious limited trajectory length effects.[29,30,38,39] Consistent with results from rotational simulations, trajectory length can affect the width of the distribution of output diffusion coefficients relative to the input width, such that individual tracked molecules may return diffusion coefficients ≈ 2 times faster or slower than the input diffusion

coefficient for experimentally realistic trajectory lengths (Fig. 3a and b). Previously, homogeneous rotational diffusion has shown broadening by up to 4 times in terms of full width at half maximum (FWHM) when trajectory length was reduced from 1000 times the rotational correlation time ($1000\tau_c$) to $10\tau_c$, with FWHM of 0.08 for the longer and 0.40 for the shorter trajectories[30]. Similarly, homogeneous translational diffusion exhibits broadening by up to a factor of 5 (FWHM of 0.10 for the longer and 0.55 for the shorter trajectories) when trajectory length is reduced from 2000 to 50 frames (10000 to 250 seconds in these simulations) (Fig. 3e). However, the majority of this broadening was captured in the change from 400 to 50 frames, or 2000 to 250 seconds.

As in rotational analysis, once significant static heterogeneity is present, width is essentially invariant to trajectory length over the range explored (35-2000 frames, or 175-10000 seconds), with distributions with an input standard deviation of 1.0 on a log scale returning distributions with standard deviations in the range of 0.90-0.98 (Fig. 3c and e). We note that while median diffusion coefficient and the width of the distribution is accurately returned independent of trajectory length for these simulations of static heterogeneity, this does not imply that individual simulated molecules return their input diffusion coefficient at short trajectory lengths (Supporting 1). Varying total time and TBF independently for homogeneous simulations reveals that output width is affected primarily by changing trajectory length in terms of total time (Supporting 2). In contrast, Fig. 3d and Fig. S2 demonstrate that varying time between frames does not affect the output distribution for cases of significant static heterogeneity, and this effect holds whether total time or number of frames is held constant (Supporting 2).

The fact that systems lacking heterogeneity experience narrowing distributions with increasing trajectory length in terms of total time while those with static heterogeneity do not suggests that monitoring distribution width over multiple trajectory lengths may be a viable way to distinguish between the presence of statistical error and static heterogeneity in wide field single particle tracking experiments. Indeed, in recent experimental studies, a decrease in width of measured D values was seen with increasing trajectory length (which in experiments is coupled to increased time between frames so that photobleaching does not occur before the end of the trajectory) exclusively in molecules far below the glass transition temperature, while molecules above T_g exhibited invariably wide distributions of diffusion coefficients across multiple trajectory lengths and TBF.[13]

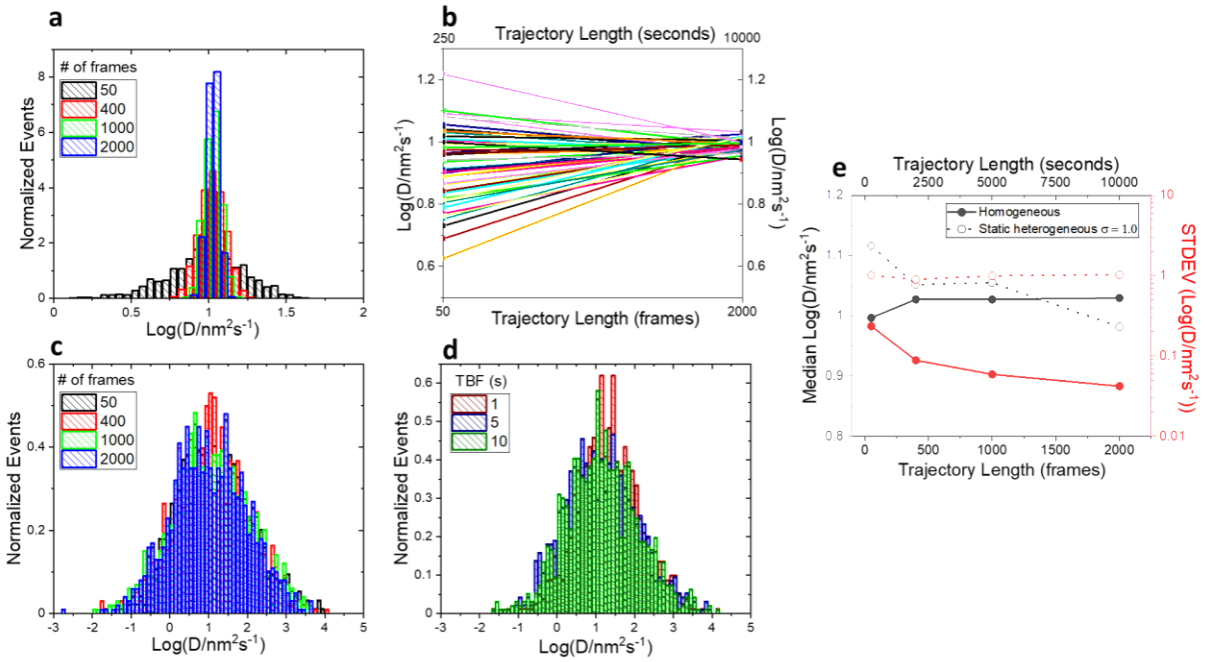

Figure 3. Noise and background-free simulations exhibiting homogeneous and static heterogeneous dynamics, all with median D_{set} = 10 nm^2s^{-1}. 1014 molecules were simulated in each case. (a) Distribution of diffusion coefficients for homogeneous simulations at varying trajectory lengths (in frames, reported in legend, as well as real time), with time between frames (TBF) for all set to 5s. (b) Diffusion coefficients for a randomly selected subset of individual molecules from the homogeneous simulation in (a) tracked for (left axis) 50 and (right axis) 2000 frames. (c) Distribution of diffusion coefficients for heterogeneous (standard deviation of log (D) = 1; designated as σ =1) simulations at varying trajectory lengths (in frames, reported in legend, as well as real time), with time between frames (TBF) for all set to 5s. (d) Distribution of diffusion coefficients for heterogeneous (σ =1) simulations for trajectory length equal to 50 frames at different time between frames (s), reported in the legend. (e) Median output diffusion coefficient and standard deviation (STDEV, σ) as a function of trajectory length for homogeneous (solid symbols) and static heterogeneous (σ = 1, open symbols) simulations. Lines are guides to the eye.

When dynamic exchange is introduced into simulations, more complex behavior is expected to be observed both in ensemble and single molecule results. For similar simulations carried out monitoring manifestations of dynamic exchange in rotational measurements of single molecules, increasing exchange led to narrowing of native input distributions and a trend towards exponential decay of rotational correlation functions, properties also found in homogeneous simulations. As such, dynamic exchange can create challenges in distinguishing between molecules with no exchange and those experiencing exchange on timescales overlapping with relaxation timescales.[29] Figure 4a demonstrates the effect of dynamic exchange on the median translational diffusion coefficients with narrow and wide seed distributions. Though all distributions had median D_{set} of 10 nm^2s^{-1}, only the narrow seed distributions retained this median value in the presence of exchange; in contrast, wide seed distributions saw a 5-fold increase in median diffusion coefficient at the fastest exchange rate (every frame, or every 5 seconds in this case). If a molecule is assigned the median diffusion coefficient, this corresponds

to exchange after exploration of ≈ 50 nm^2, a region consistent with that associated with length scale of distinct dynamical regimes in a variety of studies.[40–45] In contrast, a molecule on the fast or slow ends of the distribution would explore regions of ≈ 500 nm^2 or 5 nm^2, respectively. In addition to increasing median diffusion coefficients, Figure 4b-c demonstrate that the widths of the output trajectories decrease dramatically with increasing exchange, tending toward a delta function.

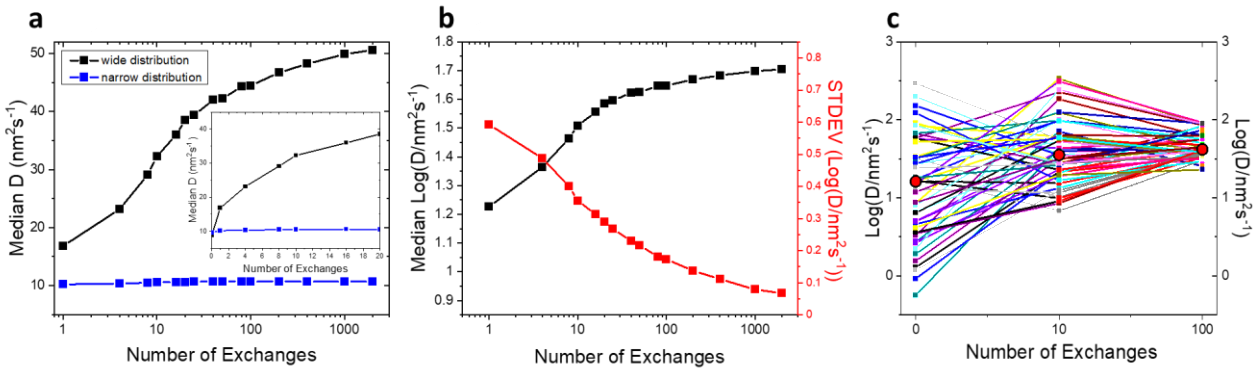

Figure 4. Simulations with molecules experiencing dynamic exchange, with median diffusion coefficients set to 10 nm^2s^{-1} and time between frames set to 5 s. 1014 molecules were simulated in each case. (a) Effect of exchange frequency on median diffusion coefficients of narrow (blue, σ = 0.2) and wide (black, σ = 0.8) seed distributions of diffusion coefficients. Inset: Initial portion of the curves, with 0 – 20 exchanges. (b) Median diffusion coefficient (left axis, black) and distribution width (right axis, red) for the wide seed distribution as a function of exchange frequency. (c) Diffusion coefficients of a randomly selected subset of individual molecules with exchange every 20 frames tracked over 2000 frames. Red circles indicate distribution medians.

The simulation's design ensures molecules are equally likely to be assigned diffusion coefficients above and below the median of the log-normal seed distribution. Hence, the increase of median diffusion coefficient with increasing exchange must have origins in the nature of the distribution and/or methods of generating trajectories. Indeed, molecules assigned large diffusion coefficients heavily influence diffusion coefficients obtained from mean square displacement calculations averaged over all molecules (quasi-ensemble MSDs), as do fast portions of an individual molecule's trajectory (Supporting 3). This phenomenon is consistent with previous suggestions and demonstrations that molecules experiencing unusually large displacements or with particularly high diffusion coefficients would lead to ensemble measurements of translational diffusion that were enhanced relative to measurements of rotational dynamics.[5,11,12] Such an argument is also relevant for individual molecules with dynamic exchange between fast and slow environments, an argument we invoked to explain the persistence of rotational-translational decoupling at the single molecule level.[13] In addition to increasing median diffusion coefficients, output distribution widths for simulations with wide seed input diffusion coefficient distributions and frequent exchange are significantly reduced, with output distributions approaching delta functions as the number of exchanges increases (Fig. 4b and c, Supporting 4). The

convergence to a single diffusion coefficient with rapid exchange introduces a degeneracy with the homogeneous case, as was found previously in rotational simulations.[30] However, the increase in median diffusion coefficients with more exchanges (in practice, experimentally, with longer trajectories in absolute time) may be used to distinguish a homogeneous case from a dynamically heterogeneous one.

Consistent with previous understanding, we find that dynamic exchange both narrows the distribution of measured diffusion coefficients and increases median and, to a greater extent, ensemble diffusion coefficient relative to the ground truth median diffusion coefficient value. However, experiments tracking single fluorescent tracer molecules in polystyrene near T_g did not reveal narrowing distributions or faster diffusion coefficients when molecules were followed for longer times.[13] As such, we considered how an experimentally realistic degree of noise and a potentially more accurate picture of dynamic exchange (in which likelihood of exchange depends on the value of the diffusion coefficient) may affect simulation findings described above.

Homogeneous and Heterogeneous Simulations With Noise

Here we explore the effects of noise on simulations of homogeneous and heterogeneous translational diffusion. As detailed in Methods, simulations can be made more similar to experiments via addition of stochastic noise as well as varying background intensity, which also has stochastic noise. For static particles, the presence of stochastic noise in the absence of background signal returned diffusion coefficients close to that of experimental results far below T_g. The addition of background signal further increased localization error above that of experiment.

When noise matching that present in wide-field experiments is added, trends in median diffusion coefficients and widths of the measured distributions remain similar to the simulations without noise, including for cases with dynamic heterogeneity (Fig. 5). Specifically, median diffusion coefficients increase with increased exchange for the heterogeneous case with a wide seed distribution but not for a narrow seed distribution, as shown in Fig. 5a. Additionally, distribution widths for wide seed distributions decrease with increasing exchange, as shown in Fig. 5b.

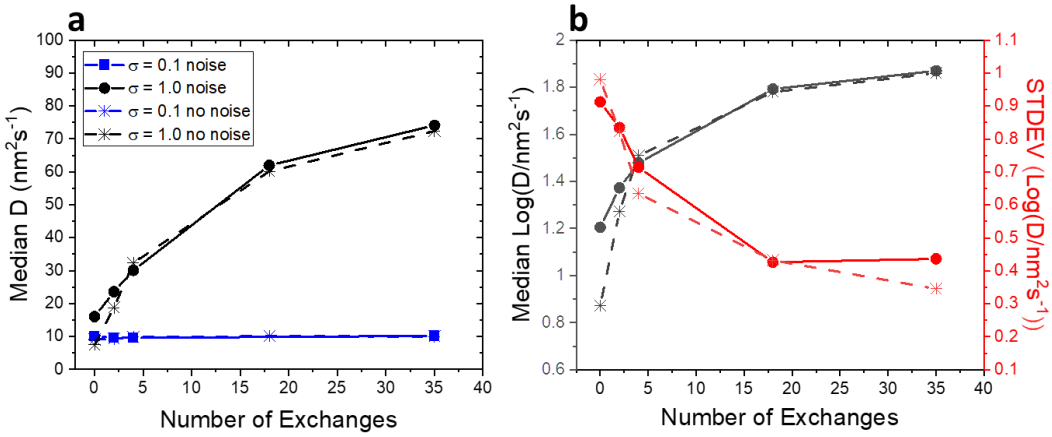

Figure 5. Simulations with noise tuned to match experimental results in Ref. 13 (see Methods) compared to simulations with no noise. 486 molecules were simulated in all cases. (a) Effect of exchange frequency on median diffusion coefficients for narrow (blue, σ = 0.1) and wide (black, σ = 1.0) seed distributions. Simulations with no noise run with the same parameters are shown in dashed lines. (b) Comparison of diffusion coefficient (left axis, black) and distribution width (right axis, red) vs. exchange frequency for simulations with a wide seed distribution (1.0 σ). Simulations with no noise run with the same parameters are shown via dashed lines. Black data points are the same in (a) and (b).

A notable feature of the experimental results presented in Ref. 13 was a decrease in median diffusion coefficient with increasing time between frames. This was an initially surprising finding given that longer time trajectories experimentally were expected to support greater likelihood for molecules to experience multiple dynamic environments, a situation typically associated with increasing diffusion coefficients. Simulations reveal that this behavior observed in experiments appears to be at least partially related to localization error that is suppressed at longer TBF, as is reflected by the trend in measured diffusion coefficient for simulated molecules with no motion but varying levels of background and noise (Fig. 6a). This behavior remains apparent, though is suppressed to a degree, in the presence of measurable diffusion coefficients in both homogeneous and static heterogeneous simulations, increasing in degree with higher background signal and with the presence of static heterogeneity (Fig. 6b, Fig. S5b,c). Notably, however, in cases of dynamic heterogeneity, this behavior is not seen, and as long as the same number of exchanges occur, median diffusion coefficients remain constant (and high relative to input diffusion coefficients) with increasing TBF regardless of background signal and noise (Fig. S5d). In these simulations, increasing TBF increases time in seconds between exchanges, and this does not affect output diffusion coefficients as long as total number of exchanges is kept constant.

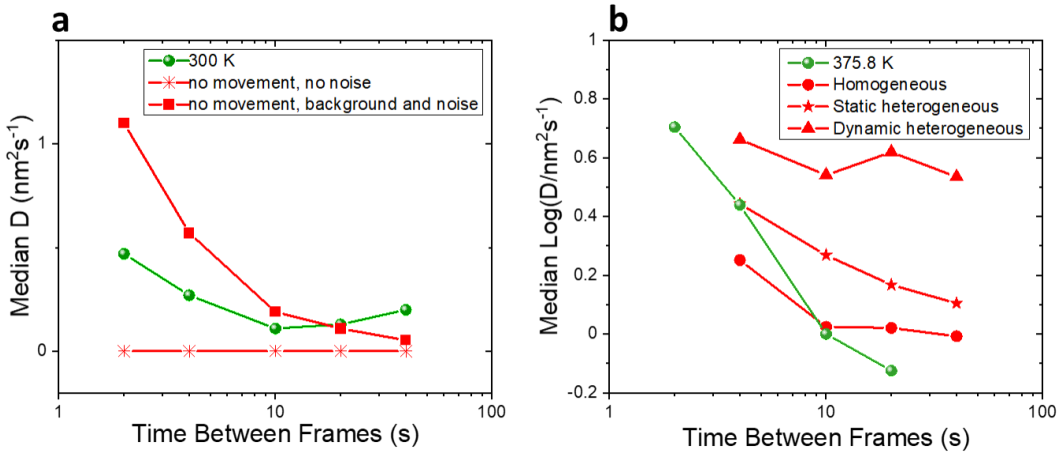

Figure 6. (a) Simulation of static molecules where all apparent motion is due to localization uncertainty and data collected from an equivalent experiment far below T_g vs. TBF. 300 K data reproduced from Ref. (13). Simulation with background and noise is shown at the highest background setting explored. (b) Homogeneous, static heterogeneous, and dynamic heterogeneous (9 exchanges) simulations at the highest background setting explored vs. experimental data collected at 375.8 K, both as a function of TBF. 375.8 K data is reproduced from Ref. 13, and shifted by a factor of 4 for ease of comparison to simulation data. Dynamic heterogeneity data obtained from simulations have particles that experience the same number of exchanges regardless of TBF. Median D vs. TBF for other noise levels is shown in Fig. S5. All simulations have 486 molecules.

The inability to fully recapitulate TBF effects seen in Ref. 13 via adding noise and background, and the loss of decrease in median D with increasing TBF for simulations including dynamic exchange suggested that the previously discussed methods of simulating heterogeneous translational diffusion do not capture the full picture of heterogeneous diffusion as it occurs in the experiments performed. To this end, the next section explores a potentially more accurate picture of dynamic exchange.

Dynamically Heterogeneous Simulations with Correlated Exchange

The previously described methods of incorporating dynamic exchange for molecules in simulated movies do so such that exchanges occur at the same frequency and at the same time for all particles. While the second of these features is clearly unrealistic, the first may also be inconsistent with dynamic exchange as it occurs in real glassy systems. In particular, we suggest that molecules traversing fast regions, consistent with high diffusion coefficients, may exchange more frequently in real time than molecules residing in regions of slow diffusion. With this in mind, simulations incorporating dynamic exchange frequency correlated with molecules' currently assigned diffusion coefficients were also performed for wide (1.0 σ) seed distributions. In this model, a molecule assigned a particularly slow diffusion coefficient from the seed distribution will take longer than average to exchange than a molecule with a higher diffusion coefficient (see

Methods for a fuller description). Results from these simulations are presented and compared to experimental data reproduced from Reference 13 in Figure 7.

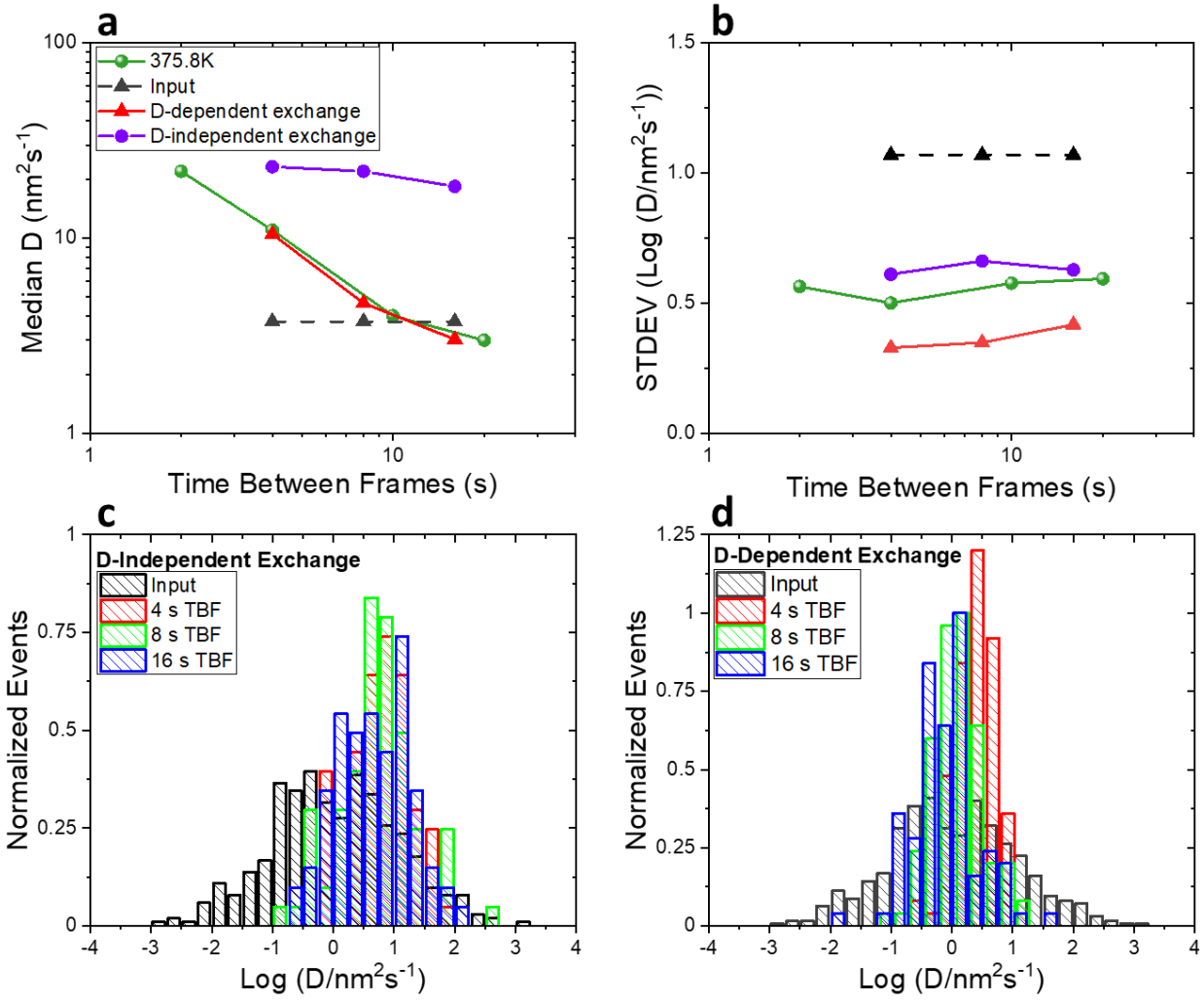

Figure 7. Simulations with dynamic exchange frequency dependent on individual molecules' current assigned diffusion coefficients (D-dependent exchange). (a) Time between frame dependence of input (black) vs. output median diffusion coefficients for D-dependent exchange (red) and D-independent exchange (purple). While medians were simulated at 1 nm^2s^{-1}, all simulation results are shifted by a factor of 4 for easier comparison to experimental data taken in polystyrene at 375.8K (green), reproduced from Reference 13. (b) Time between frames dependence of output distribution width for D-dependent (red) and D-independent (purple) exchange, with legend the same as in (a). (c) Output D distributions (colors) compared to input D distribution (black) for D-independent dynamic exchange at multiple TBF. (d) Output D distributions (colors) compared to input D distribution (black) for D-dependent dynamic exchange at multiple TBF. For all exchange conditions, the median molecule experiences the same number of total exchanges regardless of TBF. In all cases, 100 molecules were simulated.

Interestingly, when dynamic exchange frequency depends on the current assigned diffusion coefficient, the decrease in median diffusion coefficient with increasing TBF is recapitulated even in the absence of noise, and this trend persists regardless of assigned

diffusion coefficient median (Fig. 7a and Supporting 6). Additionally, diffusion coefficient distribution widths increase for increasing TBF, a feature seen to a certain extent in experiment as well (Fig. 7b). Summarizing, simulations with (uncorrelated) dynamic exchange and a fixed number of exchanges are insensitive to TBF in both median D and D distribution width (Fig. 6, Fig. 7a and b; purple, and Fig. 7c). Simulations with (uncorrelated) dynamic exchange – where number of exchanges increases with TBF – leads to increased median D and decreased distribution width compared to the input values regardless of TBF (Fig. 4, 5). None of these behaviors is consistent with experimental findings. In contrast, correlated (D-dependent) exchange results in lower median D and wider distributions with longer TBF, even as number of exchanges is kept constant per molecule (Fig. 7a,b red and Fig. 7d). It is notable that this increase in width with increasing TBF leads to output distributions that more closely match the input distributions than in other types of heterogeneous simulations.

In D-dependent exchange, we propose that the apparent decrease in median D with increasing TBF emerges because portions of trajectories associated with greater mobility, which last for short times in this type of simulation, are missed. While this can result in a decrease in median D with increasing TBF, individual molecules may not experience the same level of (or any) decrease depending on their particular trajectory (Supporting 7). To investigate this potential explanation further, molecules from the 4s TBF data set and the 16s TBF data set that were assigned the same input diffusion coefficient yet returned different output diffusion coefficients are investigated in detail in Supporting 8. It is apparent that many of the larger steps observed in the 4s TBF step size distribution are absent in the longer TBF simulation. This is a different result than for uncorrelated dynamic exchange, as for correlated exchange these large steps are associated with shorter times, and thus fewer frames, rather than persisting for equal lengths of time as those associated with low D periods. This results in large steps more likely to be missed when time between frames is increased, leading to depressed apparent diffusion coefficients. The loss of observed large steps acts counter to the tendency for dynamic exchange, as it exists in the D-independent exchange simulations, to increase diffusion coefficient values and narrow their distribution.

Conclusion

Results from simulations of single molecule translational diffusion suggest explanations for key experimental observations on translational diffusion coefficients in supercooled systems. In particular, with respect to recent single molecule measurements tracking translations of probe molecules in polystyrene near T_g, longer trajectory lengths reduce measured diffusion coefficient distribution width only for measurements far below T_g. This

finding supports the idea that the wide distributions of diffusion coefficients found in experiments performed at higher temperatures, near T_g, reflect a true wide underlying distribution. Simulations with static heterogeneity and simulations incorporating dynamic exchange in which times between exchange are uncorrelated with diffusion coefficient do not match behavior seen in experiment. Such simulations with dynamic exchange do, however, provide support for the idea that fast portions of trajectories increase diffusion coefficients obtained via time-averaged mean square displacement analysis, thus contributing to apparent rotational-translational decoupling seen in both ensemble and single molecule experiments in glassy systems. This work also shows that recent experimental results are most consistent with dynamic exchange in which there is a wide underlying heterogeneous distribution and time between exchange is correlated with diffusion coefficient. In this scenario, longer trajectories lead to an apparent decrease in diffusion coefficient, blunting the degree of translational enhancement that otherwise emerges from dynamic exchange. Taken together with experimental results presented in Ref. 13, it appears that the majority of rotational-translational decoupling in glassy systems occurs through dynamic exchange, with averaging over fast regions increasing apparent translational diffusion coefficients but not to the extent that would be expected if exchange times were uncoupled from dynamics of the spatiotemporally heterogeneous environment. The presence of a decrease in apparent diffusion coefficient with increasing time between frames only in the presence of correlated dynamic exchange suggests this physics is present in the high molecular weight polystyrene system recently investigated and may be a feature of glassy systems more generally.

Acknowledgements

This work was primarily supported by the National Science Foundation under award numbers CHE-1660392 and CHE-1954803. We thank Alec Meacham, Han Yang, and Professor Keewook Paeng for helpful discussions and Professor Dan Higgins for sharing LabView code.

Conflict of Interest

The authors have no conflicts to disclose.

Author Contributions

NLM and TR contributed equally to this work.

Data Availability

The data that support the findings of this study are available from the corresponding author upon reasonable request.

References

[1] M.D. Ediger, Annu. Rev. Phys. Chem. **51**, 99 (2000).
[2] M.T. Cicerone and M.D. Ediger, J. Chem. Phys. **104**, 7210 (1996).
[3] M.T. Cicerone, F.R. Blackburn, and M.D. Ediger, Macromolecules **28**, 8224 (1995).
[4] M.T. Cicerone, P.A. Wagner, and M.D. Ediger, J. Phys. Chem. B **101**, 8727 (1997).
[5] S. Dueby, V. Dubey, and S. Daschakraborty, J. Phys. Chem. B **123**, 7178 (2019).
[6] J. Kim and B.J. Sung, Phys. Rev. Lett. **115**, 158302 (2015).
[7] F. Puosi and D. Leporini, J. Chem. Phys. **136**, (2012).
[8] F. Puosi, A. Pasturel, N. Jakse, and D. Leporini, J. Chem. Phys. **148**, 131102 (2018).
[9] S. Sengupta, S. Karmakar, C. Dasgupta, and S. Sastry, J. Chem. Phys. **138**, (2013).
[10] M. Sharma and S. Yashonath, J. Phys. Chem. B **110**, 17207 (2006).
[11] C.D. Michele and D. Leporini, Phys. Rev. E **63**, 036701 (2001).
[12] S. Sengupta and S. Karmakar, J. Chem. Phys. **140**, 224505 (2014).
[13] N.L. Mandel, S. Lee, K. Kim, K. Paeng, and L.J. Kaufman, Nat. Commun. **13**, 3580 (2022).
[14] K. Paeng and L.J. Kaufman, Macromolecules **49**, 2876 (2016).
[15] L.J. Kaufman, Annu. Rev. Phys. Chem. **64**, 177 (2013).
[16] K. Paeng, H. Park, D.T. Hoang, and L.J. Kaufman, Proc. Natl. Acad. Sci. U. S. A. **112**, 4952 (2015).
[17] S.A. Mackowiak, T.K. Herman, and L.J. Kaufman, J. Chem. Phys. **131**, 244513 (2009).
[18] J.R. Rajian and E.L. Quitevis, J. Chem. Phys. **126**, 224506 (2007).
[19] F.R. Blackburn, C.-Y. Wang, and M.D. Ediger, J. Phys. Chem. **100**, 18249 (1996).
[20] I. Chang, F. Fujara, B. Geil, G. Heuberger, T. Mangel, and H. Sillescu, J. Non-Cryst. Solids **172–174**, 248 (1994).
[21] D.B. Hall, D.D. Deppe, K.E. Hamilton, A. Dhinojwala, and J.M. Torkelson, J. Non-Cryst. Solids **235–237**, 48 (1998).
[22] K.V. Edmond, M.T. Elsesser, G.L. Hunter, D.J. Pine, and E.R. Weeks, Proc. Natl. Acad. Sci. U. S. A. **109**, 17891 (2012).
[23] M.K. Mapes, S.F. Swallen, and M.D. Ediger, J. Phys. Chem. B **110**, 507 (2006).
[24] D.B. Hall, A. Dhinojwala, and J.M. Torkelson, Phys. Rev. Lett. **79**, 103 (1997).
[25] Y. Hwang and M.D. Ediger, J. Polym. Sci. Part B Polym. Phys. **34**, 2853 (2003).
[26] J. Singh and P.P. Jose, J. Phys. Condens. Matter **33**, 055401 (2021).
[27] M.T. Cicerone, P.A. Wagner, and M.D. Ediger, J. Phys. Chem. B **101**, 8727 (1997).
[28] S. Bhattacharyya and B. Bagchi, J. Chem. Phys. **107**, 5852 (1997).
[29] K. Stokely, A.S. Manz, and L.J. Kaufman, J. Chem. Phys. **142**, 114504 (2015).
[30] S.A. Mackowiak and L.J. Kaufman, J. Phys. Chem. Lett. **2**, 438 (2011).
[31] B.M.I. Flier, M.C. Baier, J. Huber, K. Müllen, S. Mecking, A. Zumbusch, and D. Wöll, J. Am. Chem. Soc. **134**, 480 (2012).
[32] B.M.I. Flier, M. Baier, J. Huber, K. Müllen, S. Mecking, A. Zumbusch, and D. Wöll, Phys. Chem. Chem. Phys. **13**, 1770 (2011).
[33] K.H.T. Ba, T.A. Everett, T. Ito, and D.A. Higgins, Phys. Chem. Chem. Phys. **13**, 1827 (2011).
[34] K.C. Robben, K.-H. Tran-Ba, T. Ito, and D.A. Higgins, Anal. Chem. **86**, 10820 (2014).
[35] K.-H. Tran-Ba, J.J. Finley, D.A. Higgins, and T. Ito, J. Phys. Chem. Lett. **3**, 1968 (2012).
[36] D.B. Allan, T. Caswell, N.C. Keim, and C.M. Van Der Wel, (2019).
[37] J.C. Crocker and D.G. Grier, J. Colloid Interface Sci. **179**, 298 (1996).
[38] C.Y.J. Wei, C.Y. Lu, Y.H. Kim, and D.A. Vanden Bout, J. Fluoresc. **17**, 797 (2007).
[39] C.-Y.J. Wei and D.A. Vanden Bout, J. Phys. Chem. B **113**, 2253 (2009).
[40] S.A. Reinsberg, X.H. Qiu, M. Wilhelm, H.W. Spiess, and M.D. Ediger, J. Chem. Phys. **114**, 7299 (2001).
[41] U. Tracht, M. Wilhelm, A. Heuer, H. Feng, K. Schmidt-Rohr, and H.W. Spiess, Phys. Rev. Lett. **81**, 2727 (1998).

[42] K. Kim and S. Saito, J. Chem. Phys. **138**, 12A506 (2013).
[43] B. Rijal, L. Delbreilh, and A. Saiter, Macromolecules **48**, 8219 (2015).
[44] E. Flenner, H. Staley, and G. Szamel, Phys Rev Lett **112**, 097801 (2014).
[45] S. Karmakar, C. Dasgupta, and S. Sastry, Annu. Rev. Condens. Matter Phys. **5**, 255 (2014).